EARTH SURFACE PROCESSES AND LANDFORMS
Earth Surf. Process. Landforms **37**, 157–168 (2012)
Published in 2011 by John Wiley and Sons, Ltd.
Published online 3 October 2011 in Wiley Online Library
(wileyonlinelibrary.com) DOI: 10.1002/esp.2227

Characteristics of concentrated flow hydraulics for rangeland ecosystems: implications for hydrologic modeling

Osama Z. Al-Hamdan,[1,2]* F.B. Pierson Jr,[1] M.A. Nearing,[3] J.J. Stone,[3] C.J. Williams,[1] C.A. Moffet,[4] P.R. Kormos,[5] J. Boll[2] and M.A. Weltz[6]

[1] USDA, Agricultural Research Service, Northwest Watershed Research Center, Boise, ID, USA
[2] Department of Biological and Agricultural Engineering, University of Idaho, Moscow, ID, USA
[3] USDA, Agricultural Research Service, Southwest Watershed Research Center, Tucson, AZ, USA
[4] USDA, Agricultural Research Service, US Sheep Experiment Station, Dubois, ID, USA
[5] Department of Geosciences, Boise State University, Boise, ID, USA
[6] USDA, Agricultural Research Service, Exotic and Invasive Weeds Research Unit, Reno, NV, USA

Received 31 January 2011; Revised 12 August 2011; Accepted 31 August 2011

*Correspondence to: Osama Z. Al-Hamdan, USDA, Agricultural Research Service, Northwest Watershed Research Center, 800 Park Blvd., Plaza IV, Boise, ID 83712–7716, USA. E-mail: osama.al-hamdan@ars.usda.gov

ESPL
Earth Surface Processes and Landforms

ABSTRACT: Concentrated flow is often the dominant source of water erosion following disturbance on rangelands. Because of the lack of studies that explain the hydraulics of concentrated flow on rangelands, cropland-based equations have typically been used for rangeland hydrology and erosion modeling, leading to less accurate predictions due to different soil and vegetation cover characteristics. This study investigates the hydraulics of concentrated flow using unconfined field experimental data over diverse rangeland landscapes within the Great Basin Region, United States. The results imply that the overall hydraulics of concentrated flow on rangelands differ significantly from those of cropland rills. Concentrated flow hydraulics on rangelands are largely controlled by the amount of cover or bare soil and hillslope angle. New predictive equations for concentrated flow velocity ($R^2 = 0{\cdot}47$), hydraulic friction ($R^2 = 0{\cdot}52$), and width ($R^2 = 0{\cdot}4$) representing a diverse set of rangeland environments were developed. The resulting equations are applicable across a wide span of ecological sites, soils, slopes, and vegetation and ground cover conditions and can be used by physically-based rangeland hydrology and erosion models to estimate rangeland concentrated flow hydraulic parameters. Published in 2011. This article is a US Government work and is in the public domain in the USA.

KEYWORDS: hydraulics of overland flow; rangeland; Darcy–Weisbach friction; flow velocity; flow width

Introduction

Characterization of overland flow hydraulics is paramount for rangeland process-based erosion modeling. Predicting rangeland hydrologic response is confounded by the fact that rangeland overland flow processes vary with vegetation, ground surface conditions, and hillslope topography (Pierson *et al.*, 2002, 2009). Overland flow in upland areas is a combination of concentrated flow (rills) and sheet flow. In most cases the dominant form of overland flow on rangelands with adequate vegetation cover is sheet flow. Concentrated flow emerges on steep slopes or where ground cover is sparse and is often the dominant source of water erosion following disturbance (Pierson *et al.*, 2009). Concentrated flow is deeper and faster than overland sheet flow (Julien and Simons, 1985), thus, it is important to differentiate between the two processes (Abrahams *et al.*, 1996).

There have been few studies that address the hydraulics of concentrated flow on rangeland. Roels (1984) conducted one of the earliest studies that distinguished between the hydraulic behavior of concentrated flow and sheet flow on rangelands. A rangeland hillslope in the Ardeche Basin, France, was divided into two segments; an upper section with a slope of 13·6%, and a lower section with a slope of 17·8%. Roels (1984) examined the relation of the Darcy–Weisbach resistance coefficient of the surface bed to the Reynolds number for rill (concentrated flow) and pre-rill (sheet flow) separately for each slope segment. The author concluded that the resistance coefficient relation to the Reynolds number varied considerably with respect to slope position (i.e. slope) as well as the type of flow (i.e. rill versus pre-rill). However, Roels (1984) could not address slope angle effect on flow resistance or velocity given the limited slope variation in the study design.

Abrahams *et al.* (1996) derived a multivariate equation to predict the Darcy–Weisbach roughness coefficient equation from the average size of gravels and flow discharge based on 70 field experiments for seven self-formed stony rills stabilized by a glue mixture. The rills were located on a semi-arid rangeland at Walnut Gulch, Arizona, USA with slopes ranging from 1·3% to 5·6%. Average gravel size explained most of the

variation in Darcy–Weisbach roughness coefficient. Abrahams *et al.* (1996) also derived a multivariate equation for predicting flow velocity using a stepwise regression analysis. The authors found that slope and percentage gravel significantly influenced flow velocity and were as important as discharge for controlling the velocity. However, the equations developed by Abrahams *et al.* (1996) are somewhat limited since they were developed on glued rills, and because of the narrow span of gravel cover that was used. Five out of the seven rills had gravel cover around 70%.

Nearing *et al.* (1999) analyzed the hydraulics of concentrated flow on a stony semi-arid hillslope at Walnut Gulch, Arizona with a wide range of slopes (2·6% to 30·1%). It was found that for their data, unlike Abrahams *et al.* (1996), velocity was correlated with discharge but not slope. The results agreed with cropland rill studies (Govers, 1992; Nearing *et al.*, 1997) which showed that flow velocities in rills can be predicted from discharge alone using a power relationship,

$$V = aQ^b \tag{1}$$

where V is the average flow velocity (in $m\,s^{-1}$), Q is the rill discharge (in $m^3\,s^{-1}$), and a and b are constants. Equation 1 has different values of a and b for stony semi-arid rangelands (Nearing *et al.*, 1999) versus croplands (Line and Meyer, 1988; Govers, 1992). Govers (1992) explained the absence of slope effect on flow velocities in rills by the hypotheses that the bed roughness tends to increase with slope steepness and higher erosion rates, therefore slowing the velocity. Results of Takken *et al.* (1998) suggested that slope independence of flow velocity is only true in cases where flow is capable of adjusting rill geometry, though later studies indicated that stabilization of flow velocity relative to slope also does occur on stony soils due to the long-term development of variable rock cover, and hence increased friction, as a function of slope. Over time on relatively undisturbed slopes, steeper slopes become more rocky, hence rougher (Nearing *et al.*, 1999). Govers *et al.* (2000) also showed in a flume experiment that the velocity discharge relationship is affected by the presence of rock fragments. This may explain in part why Equation 1 has different values of a and b for stony semi-arid rangeland and cropland.

The relatively few comprehensive number of studies that explain the hydraulics of concentrated flow on diverse rangeland ecosystems has resulted in the use of cropland-based equations for rangeland hydrology and erosion modeling. In physically-based models, such as the Rangeland Hydrology and Erosion Model (RHEM) (Nearing *et al.*, 2011), hydraulic parameters are used (e.g. hydraulic roughness) to route overland flow and calculate flow velocity and shear stress (Gilley *et al.*, 1990; Gilley and Weltz, 1995). Flow velocity and shear stress as well as rill width are required components to predict sediment detachment, entrainment, and transport (Line and Meyer, 1988; Nearing *et al.*, 1989). Historical rangeland model parameterization of concentrated flow processes has relied on the extensive studies conducted to describe rill or concentrated flow hydraulics on croplands (e.g. Lane and Foster, 1980; Foster *et al.*, 1984a, 1984b; Line and Meyer, 1988; Gilley *et al.*, 1990, Govers, 1992; Nearing *et al.*, 1997; Takken *et al.*, 1998; Giménez and Govers, 2001; Weisheng and Tingwu, 2002; Hessel *et al.*, 2003; Giménez *et al.*, 2004). This leads to less accurate predictions as rangelands and croplands have different soil and vegetation cover characteristics (Moffet *et al.*, 2007).

The goal of this study was to develop and provide new empirical prediction models of different rangeland concentrated flow hydraulic parameters, which can be applicable across a wide span of ecological sites, soils, slopes, and vegetation and ground cover conditions and can be incorporated into hydrology models such as RHEM. In this study we: (1) examined the hydraulics of concentrated flow using unconfined field experimental data over diverse rangeland landscapes; (2) evaluated the dependence of flow velocity, hydraulic friction, and flow path width on measured flow discharge, hillslope angle, and vegetation and ground cover characteristics; (3) developed new empirical equations for predicting flow velocity, hydraulic friction, and flow path width based on readily measureable ecological sites, soils, and vegetation characteristics.

Material and Methods

Study sites

The data used in this study were obtained from rangeland field experimental work by the US Department of Agriculture Agricultural Research Service (USDA-ARS) Northwest Watershed Research Center, Boise, Idaho. The work resulted in hundreds of experimental plots with concentrated flow. The data were collected from rangeland sites within the Great Basin region, United States. The sites are located in the states of Idaho, Nevada, Oregon, and Utah (see Figure 1). These data span a wide range of slope angles (5·6–65·8%), soil types, and vegetative cover (Tables I and II). Soil types vary from gravelly silt loam to coarse sandy loam. The vegetation community ranges from sagebrush steppe to wooded shrublands (see Romme *et al.*, 2009) in various stages of pinyon and/or juniper encroachment. Many of the sites exhibit some degree of disturbance, such as wildfire, prescribed fire, tree mastication, and/or tree cutting (see Table I). Numerous rectangular plots (approximately 4 m long by 2 m wide) were selected at each site, encompassing all treatments for the respective site. Average slope, canopy and ground cover, and micro-topography were measured for each plot (see Pierson *et al.*, 2007, 2008, 2009).

Measurement and calculation of hydraulic parameters

Overland flow was simulated on each experimental plot for a range of flow rates over near saturated surface soil conditions. Surface soils were pre-wet by artificial rainfall immediately prior to overland flow simulation (Pierson *et al.*, 2007, 2008, 2009). Overland flow was released from a concentrated source centered 4 m upslope of the plot discharge outlet (see Pierson *et al.*, 2007, 2008, 2009, 2010; Moffet *et al.*, 2007). Each inflow rate was applied for 12 minutes using a flow regulator. Except for Breaks 2004, in the early experiments (before 2006), the applied inflow rates were 3, 7, 12, 15, 21, 24 ($L\,min^{-1}$), while they were 15, 30, 45 ($L\,min^{-1}$) in the later experiments (see Table II). The plot flow velocity for each inflow rate was measured using a salt tracing method (Pierson *et al.*, 2007, 2008, 2009, 2010; Moffet *et al.*, 2007). A concentrated salt solution (calcium chloride, $CaCl_2$) was released into the fastest (as determined by visual tracer) flow path. The mean travel time of the salt solution between rill cross-sections at transects 1 and 3 m downslope of the release point was monitored instantaneously with conductivity probes. Flow velocity was calculated as the distance between conductivity probes (2 m) divided by the mean travel time of the salt solution between the 1 and 3 m transects.

The width and depth of each flow path for each rate were measured at several transects along the slope. The number and locations of transects varied within sites where the least was two transects at 1 and 3 m downslope of flow release. Only

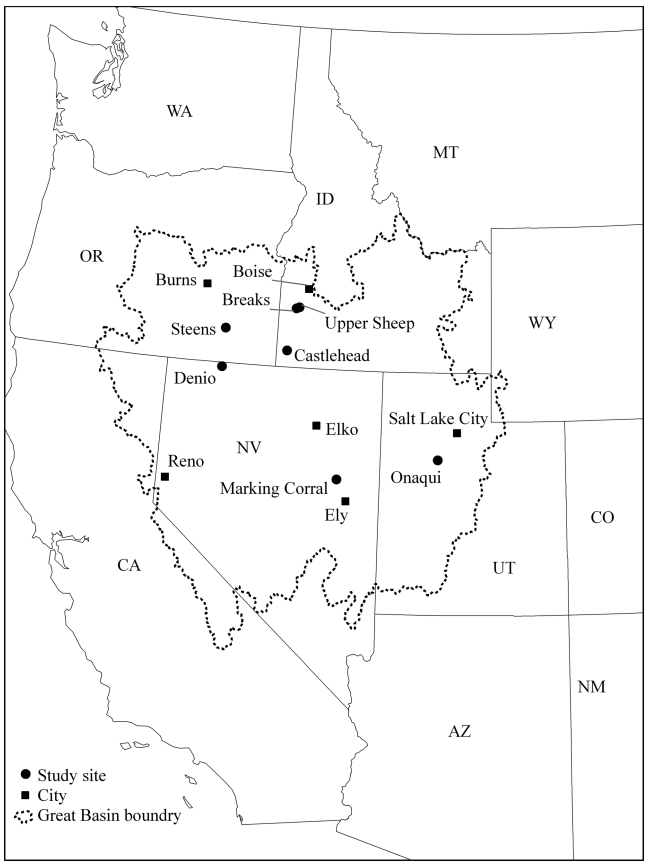

Figure 1. Geographic location of study sites distributed across the Great Basin region, USA.

the flow dimension measurements at transects 1 and 3 m were used in this study, in order to be consistent with the velocity measurements. At sites that have dimension measurements at transects 0·5, 1·5, 2·5, 3·5 m only measurements at 1·5 and 2·5 m were considered. The flow path cross-section was assumed to be rectangular. Multiple depth measurements were taken for each cross-section where the depth was calculated as the average of these measurements. The average width, depth, and hydraulic radius (R_h) of each flow path for each inflow rate was then calculated as the average of means from each cross-section. Where R_h was calculated as:

$$R_h = \frac{A}{P_{wet}} \tag{2}$$

where A is the cross-sectional area (in m^2) and P_{wet} is the wetted perimeter (in meters). In the rectangular cross-section case, R_h was calculated as:

$$R_h = \frac{wd}{(w + 2d)} \tag{3}$$

where w, d are the average width and the average depth of each flow path respectively (in meters).

Experimental runs that resulted in sheet flow (no concentrated flow) were dropped from the data set as the main objective was to examine the hydraulic characteristics of concentrated flow. In general, concentrated flow paths can be easily recognized by sight. However, sheet flow could be easily considered as several wide concentrated flow paths as it rarely submerged the soil surface entirely due to the variation of micro-topography (Smith *et al.*, 2007). Therefore, concentrated flow paths were separated from sheet flow by comparing the hydraulic radius to the flow depth for the respective flow path. If the flow path was too shallow, the depth of the flow would be negligible with respect to the width (w). In this case the denominator in Equation 3 will be approximately equal to w and R_h is approximately equal to d. In our data, if R_h and d were significantly different (d is 5% higher than R_h or more) then the flow path was considered as concentrated flow. In some cases the flow would be concentrated at the top of the plot due to scouring at the inflow release point and then start to disperse downhill changing to sheet flow. In order to avoid considering such cases as concentrated flow, the criterion was applied on each path at transects 1 and 3 m from the top of the plot. In experimental runs that formed concentrated flow paths and sheet flow paths at the same time, the case was considered as concentrated flow only if the flow path that had the largest hydraulic radius was concentrated. This last criterion was applied in order to assure that only plots dominated by concentrated flow were used in the study.

Table I. Land management treatments, dominant plant community, and soil type descriptions for rangeland field sites in this study (more detailed site descriptions can be found in site references noted at the foot of the table).

Site	State	Treatment	Plant community	Soil type
Denio[a]	NV	Burned, Untreated	Sagebrush Steppe	Ola boulder sandy loam
Breaks[b]	ID	Burned, Untreated	Sagebrush Steppe	Kanlee-Ola course sandy loam
Steens[c]	OR	Cut (long-term impact[g]), Uncut	Western Juniper	Pernty gravelly cobbly silt loam
Onaqui[d]	UT	burned, Tree mastication, Cut (short-term impact[h]) , Untreated	Utah Juniper/Sagebrush Steppe	Borvant gravely loam
Marking Corral[d]	NV	Burned, Cut (short-term impact[h]), Untreated	Single Leaf Pinyon-Utah Juniper/ Sagebrush Steppe	Segura-Upatad-Cropper gravelly loam
Castlehead[e]	ID	Burned, Cut (short- term impact[h]), Untreated	Western Juniper/Sagebrush Steppe	Mulshoe-Squawcreek-Gaib stoney loam
Upper Sheep[f]	ID	Burned, Untreated	Sagebrush Steppe	Harmel silt or Harmel silt loam

[a]Pierson et al., 2008.
[b]Pierson et al., 2009.
[c]Pierson et al., 2007.
[d]Pierson et al., 2010.
[e]McIver et al., 2010.
[f]Flerchinger and Cooley, 2000.
[g]Experiments conducted 10 years after cutting.
[h]Experiments conducted within one year after cutting.

Table II. Summary of sampling frequency, simulated flow rates, and hillslope gradients for each study site by study year.

		Number of plots							
Site	Year	Burned	Untreated	Cut (short-[a] or long-term[b] impact)	Uncut	Tree mastication	Total	Inflow rate (L min^{-1})	Slope
Denio	2000	18	18	—	—	—	36	7,12,15,21,24	27·9–65·8
	2001	20	16	—	—	—	36	7,12,15,21,24	23·4–51
	2002	18	17	—	—	—	35	7,12,15,21,24	26·5–47·8
	2003	16	—	—	—	—	16	7,12,15,21,24	26·1–36
Breaks	2002	8	8	—	—	—	16	3,7,12,15,21,24	34·7–49·1
	2003	8	—	—	—	—	8	3,7,12,15,21,24	34·7–48·6
	2004	8	—	—	—	—	8	3,7,12,15,21,24,48	33–55·9
	2005	8	—	—	—	—	8	3,7,12,15,21,24	38–47
Steens	2001	—	—	8	8	—	16	3,7,12,15	15·7–22
Onaqui	2006	—	36	—	—	—	36	15,30,45	9·1–23·6
	2007	12	—	12	—	8	32	15,30,45	9–25·9
	2008	12	4	—	—	—	16	15,30,45	12–26·1
Marking Corral	2006	—	24	—	—	—	24	15,30,45	5·6–12·5
	2007	12	—	12	—	—	24	15,30,45	6–13·3
	2008	12	6	—	—	—	18	15,30,45	7–21·3
Castle Head	2008	12	12	6	—	—	30	15,30,45	13·1–23·4
Upper Sheep	2007	—	20	—	—	—	20	15,30,45	12·4–38·7
	2008	12	—	—	—	—	12	15,30,45	20–39·3
All sites		176	161	38	8	8	391		5·6–65·8

[a]Experiments conducted within one year after cutting.
[b]Experiments conducted 10 years after cutting.

High vegetation cover (i.e. basal plant and plant residue cover more than 75% of plot), at sites such as Denio's unburned sites made measurements of the flow path width and depth in experimental runs more difficult than at sites with low or no vegetation cover. We evaluated width and depth measurement errors for each experimental run by comparing measured flow discharge to discharge calculated as the product of measured velocity and flow area (measured width multiplied by measured depth). Observations from densely covered sites were dropped when the respective measurement error was outside 95% of the range of measurement error for all experimental runs. The total number of experimental runs that generated runoff was 756, where 391 were considered concentrated flow according to the applied criteria. Most of the concentrated flow observations were from the burned or steep sloped sites or both (see Table III).

The overland flow discharge for each experimental run was calculated as the average of the inflow rate and the outflow rate of a plot. While the inflow rate was controlled and measured by the flow regulator, the outflow discharge rate was derived from timed runoff samples which were collected in bottles or buckets at the exit of the plot (see Pierson *et al.*, 2007, 2008, 2009, 2010). The outflow discharge rate was calculated as sample volume divided by the collection time. For each experimental run, timed runoff samples were collected and the average runoff value was calculated.

Flow path discharge was considered to be equal to the measured plot overland flow discharge when only one concentrated flow path was formed in the experimental run. In this case, the measured velocity corresponds to the respective flow path discharge. However, in the case where multiple concentrated flow paths formed in the plot during the experiment, the velocity was only measured at the fastest flow path which had the largest hydraulic radius. In order to find the flow discharge in the flow path that corresponded to the measured velocity, the total overland flow discharge was distributed to the flow paths based on their hydraulic radius. Flow paths with higher hydraulic radius had more capacity for flow discharge as they had smaller wetted perimeter for the same cross-section area. In order to attribute flow discharge rates to the multiple rills of an experiment where only total flow discharge for all rills was measured, we applied the conveyance concept that is used in the Hydrologic Engineering Center's HEC-2 model for balancing the discharge between different channel components

Table III. Number of experimental runs that formed at least one concentrated flow path for each study site by study treatment (figures inside parenthesis indicate the number of experimental runs that only formed one concentrated flow path).

	Number of concentrated flow observations					
Site	Burned	Untreated	Cut (short-[a] or long-term[b] impact)	Uncut	Tree mastication	Total
Breaks	130 (3)	18	—	—	—	148 (3)
Castlehead	—	1 (1)	1 (1)	—	—	2 (2)
Denio	135 (9)	32 (12)	—	—	—	167 (21)
Marking Corral	15 (2)	11	3 (1)	—	—	29 (3)
Onaqui	1	5	—	—	2	8
Steens	—	—	7	14	—	21
Upper Sheep	13 (3)	3	—	—	—	16 (3)
All sites	294 (17)	70 (13)	11 (2)	14	2	391 (32)

[a]Experiments conducted within one year after cutting.
[b]Experiments conducted 10 years after cutting.

(US Army Corps of Engineers, 1993). The concept uses Manning's equation for calculating the conveyance factor (K) for each component and then distributes the total flow rate proportionally to each channel component based on its K value. With the assumption that each flow path had a similar hydraulic roughness value and slope, Manning's equation takes the form

$$Q = \frac{1}{n} A R_h^{2/3} S^{1/2} = K \frac{S^{1/2}}{n} \quad (4)$$

where n is manning's roughness parameter (in s $m^{-1/3}$), A is the cross-sectional area (in m^2) of the flow path, S is the average slope of the plot, and R_h is the hydraulic radius (in meters) and

$$K = A R_h^{2/3} \quad (5)$$

The flow discharge was proportionally distributed to the flow paths according to their conveyance factor. For instance, an individual flow path with twice the conveyance factor as a second flow path would have twice the share of the collective flow.

The use of conveyance concept of HEC-2 model for distributing the total flow discharge is approximate, but it strengthens the resulting equations by allowing the use of a greater number of observations with diverse slope and ground cover to the regression analysis. As Table III shows, the number of observations from the experiments that formed only one concentrated flow path is 32. Most of those observations were located at one site (Denio).

Reynolds number (R_e), Froude number (F_r) and Darcy–Weisbach friction factor (f) of the fastest flow path were calculated as:

$$R_e = \frac{4 V R_h}{\upsilon} \quad (6)$$

$$F_r = \frac{V}{\sqrt{g \frac{A}{w}}} \quad (7)$$

$$f = \frac{8 g R_h S}{V^2} \quad (8)$$

where V is the measured velocity (in m s^{-1}), υ is the kinematic viscosity (in m^2 s^{-1}), S is the average slope of the plot, g is the acceleration due to gravity (in m s^{-2}), and R_h, w, and A are the hydraulic radius (in meters), the width (in meters), and the cross-sectional area of the fastest flow path (in m^2) respectively. In order to make sure that Q, V, w, and d were internally consistent with one another, Equations 6–8 were calculated based on measured Q, V, and w (i.e. a calculated d from measured Q, V, and w was used instead of the field measured depth). The rationale for this was based on our field experience indicating that the measured depth values are relatively uncertain.

Finally the hydraulic parameters were also calculated assuming triangular and parabolic cross-sections. The hydraulic radii for the triangular and parabolic cross-sectional flow path are functions of flow surface width and the maximum depth. In both cases the hydraulic radius was calculated using the calculated maximum depth of the cross-section from the measured Q, V, and w instead of the field measured maximum depth.

Statistical analysis

The SAS software was used for all statistical analyses. The general linear model was used to test the significance of differences between relationships among any groups of data sets. Multiple stepwise linear regression analysis was used to derive all the relationships between the hydraulic parameters. Prior to this analysis, values of V, f, and w were log transformed (base 10) to address deviation from normality as well as to improve homoscedasticity and linearity (Allison, 1999). In addition to the ordinary least squares (OLS) regression, reduced major axis (RMA) regression was used to develop the relationship between velocity and flow discharge and width and flow discharge. Analysis of variance was used to test whether equation coefficients like a and b in Equation 1 were different than those determined by previous studies. In order to assess the validity of the conveyance concept approximation, a paired t-test was used for comparing the predicted values of the resulting equations obtained using the conveyance concept approximation with observations from experiments where the conveyance approximation was not used, i.e. 32 data points of experiments that only formed one concentrated flow path. Significance level of 0·05 was used for all statistical tests including the criteria for including the variables in the multiple regressions.

Sensitivity analysis

Sensitivity analyses of the resultant hydraulic predictive equations were performed to determine the robustness of the resultant equations for use in process-based runoff models. The parameters selected for the analysis were Q, S, and the vegetation and ground cover attributes fractions (i.e. basal plant, plant residue, and rock). The ranges of the parameters were selected to cover the entire observation space in this study. Selected Q ranged from 0·00001 m^3 s^{-1} to 0·00091 m^3 s^{-1} with the increment used in the sensitivity analysis of 0·00006 m^3 s^{-1}, selected S ranged from 0·05 to 0·7 with an increment of 0·05, and selected vegetation and ground cover ranged from 0 to 1 with an increment of 0·1. For the Q parameter, the model response was calculated by setting S to an average value and the total of vegetation and ground cover equal to 0·5 (i.e. basal plant = 0·1, plant residue = 0 3, and rock = 0·1), these cover values were close to the average values of the experimental data from which the equations were developed from. For the S parameter, the model response was calculated by setting Q at the average value and the total of vegetation and ground cover equal to 0·5 (i.e. basal plant = 0·1, plant residue = 0·3, and rock = 0·1). For basal plant, plant residue, and rock the model response was calculated by setting S and Q parameters at average values and setting all vegetation and ground cover attributes except for the studied parameter at zero. The model response was also calculated by setting all parameters at their ranges' boundaries.

The root mean square error (RMSE) was used to test the sensitivity of the derived velocity equations to cross-sectional flow path shape. The RMSE was calculated for the velocity model responses when assuming rectangular, triangular, and parabolic shapes as:

$$\mathrm{RMSE} = \sqrt{\frac{\sum_{i=1}^{n} (M_i - O_i)^2}{n}} \quad (9)$$

where M is the model response, O is the observed value, and n is the total number of observations.

Results

Hydraulics regime

The Reynolds number and Froude number (Figure 2) indicate the data set is indicative of a concentrated flow hydraulic regime. The Reynolds number ranged from 573 to 18 915, and Froude number ranged from 0·033 to 2·13. Reynolds numbers are within the range of other rill experimental data (e.g. Nearing *et al.*, 1997). Figure 2 also shows that with an exception of few observations, all of the experimental data were in the subcritical range (i.e. Froude number < 1). The observed hydraulics regime agrees with the hypothesis by Grant (1997) that, in general, the interactions between the water surface and the bed structure in mobile channels tend to prevent the Froude number from exceeding one for long distances and periods of time. Flow regime was also concurrent with Giménez and Govers' (2001) experiments in eroded rills which showed that the Froude number remained roughly constant and near critical for a wide range of slope and discharge conditions.

Except for the Steens uncut site, which did not show any significant trend, the relationship between f and R_e was consistent among all sites and treatments as it shows a decrease in f as R_e increases. Figure 3 shows that a general f–R_e relation can be developed from the entire data of this study regardless of the roughness elements. The result contrasts with other studies that showed f and R_e do not indicate consistency or single monotonic relationship (e.g. Roels, 1984; Abrahams *et al.*, 1990; Nearing *et al.*, 1997). Abrahams *et al.* (1990) proposed that such inconsistency is a result of progressive inundation of ground surfaces with different configurations, where resistance will increase with flow rate as wetted surface area increases, and starts to decrease with R_e after it is totally submerged. Hence, the negative correlation between R_e and f agrees with the assumption that the selected data were obtained from concentrated flow experiments where a total submergence is predominant in the flow path.

The average measured width of the flow paths ranged from 3·5 cm to 54·5 cm with a median value of 12 cm. The average depth of the flow ranged from 0·23 cm to 6·65 cm with a median value of 1·02 cm. The hydraulic radius ranged from 0·22 cm to 3·72 cm with a median value of 0·86 cm. The average velocity ranged from 0·019 m s^{-1} to 0·45 m s^{-1} with a median value of 0·119 m s^{-1}. The average of the total friction factor ranged from 0·43 to 1480 with a median of 15·8.

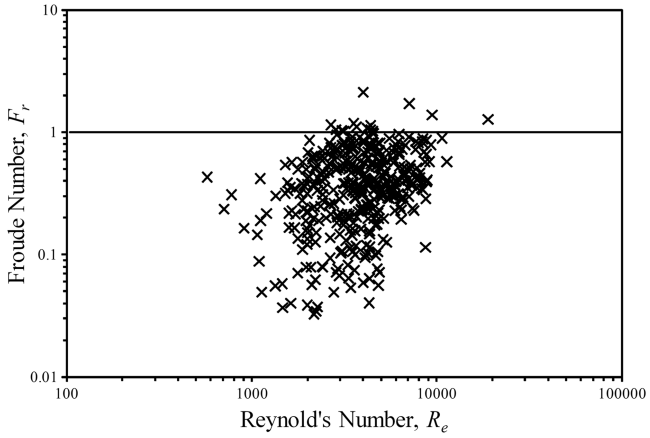

Figure 2. Froude number (F_r) and Reynolds number (R_e) for the experimental data.

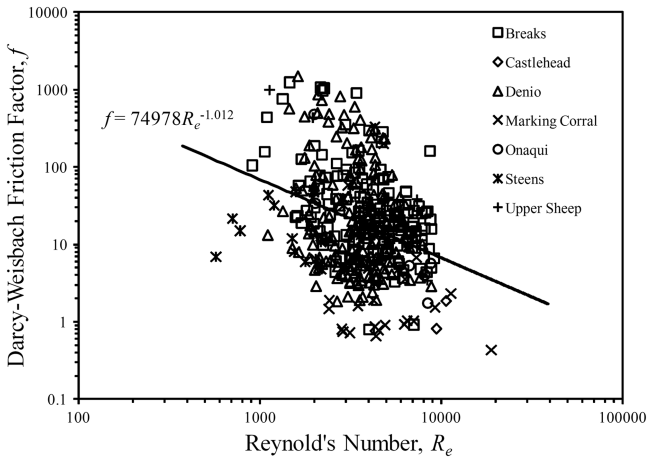

Figure 3. Darcy–Weisbach friction factor (f) as a function of Reynolds number (R_e) for all study sites.

Flow velocity

The overall dependence of flow velocity on discharge was weak, but the variability of velocity when partitioned by percentage of bare soil was well explained by a power function inclusive of both discharge and slope as independent variables. The regression analysis between logarithm of velocity and logarithm of discharge yields

$$\log V = -0.025 + 0.245 \log Q \quad (n = 391, R^2 = 0{\cdot}07) \quad (10)$$

The small correlation coefficient for the velocity and discharge relationship was not surprising. Takken *et al.* (1998) suggested that Equation 1 is a poor predictor when non-erodible vegetation and ground cover elements are present. Velocity was positively correlated ($\alpha = 0{\cdot}05$) with the discharge, hydraulic radius, slope, and the percentage of bare soil; and negatively correlated with percentage of litter cover, percentage of plant basal cover, and percentage of rock cover. Therefore, the data were further analyzed by dividing the whole dataset into four groups based on their percentage of bare soil (0% to 25%, 25% to 50%, 50% to 75%, and 75% to 100%.). A general linear test shows that the values of coefficients b in Equation 1 among the four groups are significantly different ($\alpha = 0{\cdot}05$). A step-wise multiple regression analysis for a power function for predicting logarithm of velocity as a function of logarithm of discharge and logarithm of slope was performed. The regression analysis for each group shows that the less vegetation and rock cover the better predictor the power relation between velocity and discharge would be (see Equations 11–15 in Table IV). These results agree with the Takken *et al.* (1998) suggestion that the more non-erodible elements found in the flow path the less chance that Equation 1 would be a good predictor. However, even for sites with more than 75% of bare soil, the flow discharge still does not explain most of variance (partial $R^2 = 0{\cdot}33$). Moreover, Table IV shows that the velocity–slope correlation increases for sites with less cover. Adding slope in the regression analysis for the sites with more than 75% bare soil increases the explained variance by 0·33. In addition, our results show that, within the scope of the data in this study, slope gradient had more influence on rock cover fraction in sites with less vegetation cover as seen in Equations 16–20 in Table V.

In order to determine if slope indirectly affected the velocity along with the rock cover, the variable slope used to generate the equations in Table IV was replaced by the variable rock cover. A multiple regression analysis for predicting velocity as a

Table IV. Multiple regressions equations to estimate velocity as a function of flow discharge (Q) and slope (S) for data groups based on their percentage of bare soil.

Percentage bare soil	Regression equation	Equation number	n	Coefficient of determination	
				R^2	log S partial R^2
0–100%	$\log V = -0.025 + 0.245 \log Q$	11	391	0·07	—
0–25%	$\log V = 0.3 + 0.387 \log Q$	12	77	0·13	—
25–50%	$\log V = 0.662 + 0.468 \log Q - 0.18 \log S$	13	124	0·3	0·02
50–75%	$\log V = 0.805 + 0.408 \log Q + 0.21 \log S$	14	109	0·52	0·05
75–100%	$\log V = 1.15 + 0.381 \log Q + 0.862 \log S$	15	81	0·66	0·33

Table V. Relationship for rock cover fraction (rock) as a function of slope (S) for data groups based on their percentage of bare soil.

Percentage bare soil	Regression equation	Equation number	n	Coefficient of determination (R^2)
0–100%	$rock = -0.094 - 0.27 \log S$	16	171	0·24
0–25%	$rock = -0.18 - 0.456 \log S$	17	40	0·32
25–50%	$rock = -0.07 - 0.262 \log S$	18	61	0·23
50–75%	$rock = -0.049 - 0.16 \log S$	19	43	0·53
75–100%	$rock = -0.082 - 0.194 \log S$	20	27	0·67

Table VI. Multiple regressions equations for estimating velocity (V) as a function of flow discharge (Q) and rock cover (rock).

Percentage bare soil	Regression equation	Equation number	n	Coefficient of determination	
				R^2	Rock partial R^2
0–100%	$\log V = -0.025 + 0.245 \log Q$	21	391	0·07	0·06
0–25%	$\log V = 0.3 + 0.387 \log Q$	22	77	0·13	—
25–50%	$\log V = 0.946 + 0.519 \log Q$	23	124	0·28	—
50–75%	$\log V = 0.569 + 0.375 \log Q$	24	109	0·47	—
75–100%	$\log V = 0.999 + 0.433 \log Q - 4.766 rock$	25	81	0·66	0·38

function of flow discharge and rock cover fraction was performed resulted in Equations 21–25 (Table VI). It can be seen that slope gradient was only replaced by rock cover in sites with minimum vegetation cover. This result can be explained by the fact that other hydraulic roughness factors such as vegetation cover and bed form roughness also vary with slope.

Tables IV and VI show that prediction of velocity by using only flow discharge has a more accurate fit for sites with more bare soil and less vegetation cover regardless of the impact of other factors. In order to validate this assumption, a multiple regression equation between velocity as a dependent variable and discharge, slope, vegetation cover, and rock cover as independent variables was developed using the experimental data taken in 2000 for the burned site at Denio, which has an average of 95% bare soil, yielding the equation

$$V = 10Q^{0.441} \quad (n = 53, R^2 = 0{\cdot}68) \tag{26}$$

A multiple regression equation between the logarithm of velocity as a dependent variable and discharge, slope, vegetation cover, and rock cover as independent variables was developed for predicting velocity from flow discharge for different vegetation and rock cover levels

$$\log V = -0.921 - 0.566\text{res} - 0.615\text{bascry} - 0.582\text{rock} + 974Q + 0.19S \quad (n = 391, R^2 = 0{\cdot}47) \tag{27}$$

where res, bascry, and rock are the fractions of litter cover, basal plant and cryptogam cover, and rock cover to the total ground cover respectively. Considering the diversity of the field experimental data, Equation 27 could be used as a new method to predict concentrated flow velocity directly without using a friction factor value as the friction elements are already embedded in the equation.

A paired t-test was used to compare the prediction of Equation 27 with observations from experiments that only formed one concentrated flow path. With a p-value of 0·18, the results showed that values estimated using Equation 27 and the observed values are not significantly different. In the case where bare soil percentage is available while the fractions of the attributes of ground cover are not, the velocity can be estimated using only the percentage of bare soil as follows

$$\log V = -1.505 + 0.583 bare + 980Q + 0.195S \quad (n = 391, R^2 = 0{\cdot}47) \tag{28}$$

where bare is the bare soil fraction of the total area.

Hydraulic friction

Hydraulic friction was negatively correlated with flow discharge and percentage bare soil; and was positively correlated with the presence of vegetation cover and slope. A stepwise regression analysis between logarithm of f as a dependent variable and vegetation cover, and rock cover as independent variables yielded the following equation

$$\log f = 0.524 + 1.54res + 1.934bascry \quad (n = 171, R^2 = 0{\cdot}44) \tag{29}$$

Adding flow discharge to the regression analysis in Equation 29 improved predictive capability, yielding the equation

$$\log f = 0.832 + 1.439res + 1.776bascry - 1440Q \quad (n = 391, R^2 = 0{\cdot}46) \tag{30}$$

Adding slope to the regression analysis in Equation 30 also improved predictive capability, yielding the equation

$$\log f = 0.235 + 1.368res + 1.778bascry + 1.292rock - 1499Q + 1.722S \quad (n = 391, R^2 = 0{\cdot}52) \tag{31}$$

A paired *t*-test was used to compare the prediction of Equation 31 with observations from experiments that only formed one concentrated flow path. With a *p*-value of 0·21, the results showed that values estimated using Equation 31 and the observed values are not significantly different.

In the case where partitioning of friction factor is not important, the total friction factor can be estimated using only the percentage of bare soil as follows

$$\log f = 1.734 - 1.511bare - 1624Q + 1.734S \quad (n = 391, R^2 = 0{\cdot}52) \tag{32}$$

where bare is the bare soil fraction of the total area.

Flow path widths

Flow path width was moderately dependent on flow discharge and hillslope angle. The concentrated flow width for all sites combined was positively correlated ($\alpha = 0{\cdot}05$) with the discharge, percentage of litter cover, percentage of rock cover, and percentage of basal plant cover; and negatively correlated with the slope and percentage of bare soil. Therefore, multiple stepwise regression was performed using all sites experimental data to develop an equation to predict the concentrated flow width, where *Q*, *S*, rock, res, and bascry are independent variables, yielding

$$\log w = -0.894 + 772Q - 0.762S + 0.258res + 0.202bascry \quad (n = 391, R^2 = 0{\cdot}4) \tag{33}$$

Paired *t*-test was used to compare the prediction of Equation 33 with observations from experiments that only formed one concentrated flow path. With a *p*-value of 0·26, the results showed that values estimated using Equation 33 and the observed values are not significantly different.

Omission of the res and bascry variables and replacement of *Q* and *S* by logarithm of *Q* and logarithm of *S* yields

$$\log w = 0.391 + 0.389\log Q - 0.396\log S \quad (n = 391, R^2 = 0{\cdot}37) \tag{34}$$

The negative correlation between slope and width was expected since the flow tends to concentrate on steeper slopes and to disperse on gentle slopes. This relationship is clearly evident with all observations given that concentrated flow occurred on less than 19% of the gently sloping sites (slope 20%) and on more than 58% of the steep sites (slope > 20%). Furthermore, omission of logarithm slope in Equation 34 reduces the R^2 value by 9% and yields

$$\log w = 0.838 + 0.45\log Q \quad (n = 391, R^2 = 0{\cdot}28) \tag{35}$$

Changing Equation 35 in the power functional form $w = aQ^b$ suggested by Gilley *et al*. (1990) yields

$$w = 6.89Q^{0.45} \tag{36}$$

Flow path width was negatively correlated with bare soil area. Replacing vegetation cover in Equation 31 with bare soil fraction yields

$$\log w = -0.677 + 708Q - 0.694S - 0.23bare \quad (n = 391, R^2 = 0{\cdot}39) \tag{37}$$

Multiple stepwise regressions performed using experimental data for each site separately showed no correlation between flow widths and slopes.

Sensitivity analysis

The responses of *V* in Equation 27 varied from 0·03 at the bascry highest value of one and *Q* and *S* lowest values, to 1·254 at 100% bare soil and *Q* and *S* highest values (see Table VII). The response of *f* in Equation 31 varied from 0·1 at 100% bare soil, *Q* highest value, and *S* lowest value; to 1597·4 at bascry highest value, *Q* lowest value, and *S* highest value. The response of *w* in Equation 33 varied from 0·038 m at 100% bare soil, *Q* lowest value, and *S* highest value; to 0·938 at bascry highest value, *Q* highest value, and *S* lowest value. The sensitivity of the responses to the change of the variables did not change significantly within the full space of parameters. For instance, changing *Q* from 0·00001 $m^3 s^{-1}$ to 0·00091 $m^3 s^{-1}$ increases *V* by a factor of 7·5 regardless at what values the other variables were fixed.

The values of *V* in Equation 27 did not change with the change of cross-sectional shape as it is independent of flow path dimensions. The results from Equation 27 had a RMSE of 0·046 $m s^{-1}$. However, when *V* is calculated by substituting Equation 31 into Equation 8, the results depend on the cross-sectional shape as Equation 31 will have different coefficients for different cross-sectional shapes while Equation 8 depends on flow path dimensions represented by the hydraulic radius. However, the results reveal that in general the values of *V* obtained from Equation 8 showed relatively small differences when assuming different shapes (Table VIII). The calculated values of *V* from Equation 8 ranged from 0·017 $m s^{-1}$, 0·016 m s^{-1}, 0·016 $m s^{-1}$ to 0·7 $m s^{-1}$, 0·703 $m s^{-1}$, and 0·837 $m s^{-1}$ for rectangular, triangular and parabolic cross-sectional shapes respectively (Table VIII). The RMSE values were 0·059 $m s^{-1}$, 0·058 $m s^{-1}$, and 0·061 $m s^{-1}$ for rectangular, triangular, and parabolic cross-sectional shapes respectively.

Discussion

Flow velocity

Our results for flow velocity are consistent with Takken *et al*. (1998), which suggested that the ability of flow discharge to predict velocity improves in the absence of non-erodible roughness elements (plant, residue, stones). However, the results of this study indicate that the dependency of velocity on slope also increases as non-erodible roughness elements decrease. The absence of slope effect on flow velocities was explained in the literature by the hypotheses that steeper rills

Table VII. Values of variables and their corresponding velocity, friction factor, and width calculated by the predictive equations.

Flow discharge, Q (m^3 s^{-1})	Slope, S	Basal plant, bascry	Plant residue, res	Rock cover, rock	Velocity,[a] V (m s^{-1})	Friction factor,[a] f	Width,[a] w (m)
0·00046	0·05	0·1	0·3	0·1	0·177	2·2	0·332
0·00046	0·7	0·1	0·3	0·1	0·235	29·4	0·106
0·00046	0·375	0	0	0	0·397	1·6	0·150
0·00046	0·375	1	0	0	0·096	93·2	0·238
0·00046	0·375	0	1	0	0·108	36·2	0·271
0·00046	0·375	0	0	1	0·104	30·4	0·150
0·00001	0·05	0	0	0	0·125	2·0	0·119
0·00091	0·05	0	0	0	0·944	0·1	0·589
0·00001	0·05	1	0	0	0·030	121·4	0·190
0·00091	0·05	1	0	0	0·229	5·4	0·938
0·00001	0·375	0·1	0·3	0·1	0·074	38·3	0·084
0·00091	0·375	0·1	0·3	0·1	0·559	1·7	0·417
0·00001	0·7	1	0	0	0·040	1597·4	0·061
0·00091	0·7	1	0	0	0·304	71·5	0·300
0·00001	0·7	0	0	0	0·167	26·6	0·038
0·00091	0·7	0	0	0	1·254	1·2	0·188

[a]Velocity, friction factor, and width calculated by Equation 27, Equation 31, and Equation 33 respectively.

Table VIII. Values of variables and their corresponding velocity calculated using Equation 8 for f obtained from different Equation 31 forms based on cross-sectional shape assumption.

Flow discharge, Q (m^3 s^{-1})	Slope, S	Basal plant, bascry	Plant residue, res	Rock cover, rock	Velocity, V (m s^{-1})		
					Rectangular	Triangular	Parabolic
0·00046	0·05	0·1	0·3	0·1	0·195	0·188	0·232
0·00046	0·7	0·1	0·3	0·1	0·148	0·147	0·133
0·00046	0·375	0	0	0	0·321	0·320	0·317
0·00046	0·375	1	0	0	0·053	0·053	0·053
0·00046	0·375	0	1	0	0·091	0·095	0·091
0·00046	0·375	0	0	1	0·069	0·069	0·064
0·00001	0·05	0	0	0	0·105	0·105	0·107
0·00091	0·05	0	0	0	0·674	0·638	0·837
0·00001	0·05	1	0	0	0·019	0·020	0·021
0·00091	0·05	1	0	0	0·067	0·067	0·071
0·00001	0·375	0·1	0·3	0·1	0·070	0·071	0·067
0·00091	0·375	0·1	0·3	0·1	0·278	0·282	0·290
0·00001	0·7	1	0	0	0·017	0·016	0·016
0·00091	0·7	1	0	0	0·090	0·079	0·096
0·00001	0·7	0	0	0	0·140	0·141	0·137
0·00091	0·7	0	0	0	0·700	0·703	0·693

tend to form more knickpoints and increase the roughness of the surface due to the erosion process, therefore slowing the velocity and counteracting the slope increase (Govers, 1992; Nearing *et al*., 1997; Giménez and Govers, 2001). In the case of consolidated soil containing rock fragments, Nearing *et al*. (1999) suggested that the increase of roughness that counteracts the slope effect is due to erosion processes which cause the rock concentrations to be greater at steeper slopes. The positive correlation in that study between the slope and rock cover agreed with many previous studies on rock cover (e.g. Simanton *et al*., 1994; Poesen *et al*., 1998). However, the measurements of rock cover in our study show in general negative correlation with slope gradient. Rock cover did not increase with slope steepness because these data were collected across a wide geographic area (Figure 1) and hence factors other than slope, such as hillslope aspect, soil type, and land use determined the rock cover (Poesen *et al*., 1998). Both this study and that of Nearing *et al*. (1999) with respect to the rock cover versus slope gradient relationship indicate that the rock cover fraction had a significant impact on velocity.

Moreover, in our data, rock showed even stronger negative correlation with slope in sites with minimum vegetation cover. One would expect that the relationship between slope and rock cover would be positively correlated since steeper hillslopes tend to erode more, exposing the non-erodible rock. This would be true with undisturbed rangeland, where the erosion process reaches a steady state status. However, in newly disturbed rangeland, like the burned sites in this study, the surface soil layer could still cover the rock layers. In such cases, velocity would be dependent on slope until the rock is uncovered. Another explanation for the significant velocity dependence on slope in this study would be the wide range of slopes of the experimental sites. At high difference in slopes, the slope impact would be too large to be counteracted by the change in surface roughness due to erosion.

Velocity at the Denio site was well described by discharge alone (Equation 26). The reason why the slope or rock fragment did not have an impact on velocity at this site is the fact that there was no variation in slope or rock cover fraction that would show an impact on the equation at a 95% bare soil site. Equation 26 is similar to that reported by Nearing *et al*. (1999) who used data from a semi-arid hillslope (see Figure 4), where the data of Denio site did fall within the envelope of data reported by Nearing *et al*. (1999). This result emphasizes the

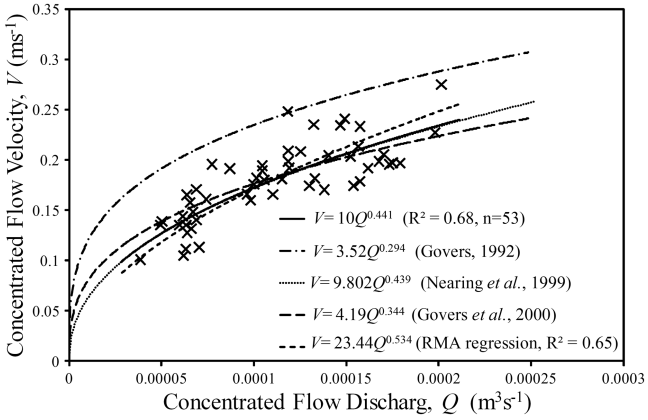

Figure 4. Power relationship for concentrated flow velocity as a function of flow discharge on 95% bare soil site, Denio ($n = 53$), compared to relationships developed by previous studies.

conclusion of Takken *et al.* (1998) that velocity can be explained by discharge alone (Equation 1) only when the site is predominantly bare soil. In addition, as can be seen in Figure 4, RMA regression shows the same result where velocity at the Denio site was well described by discharge alone. This is important as RMA regression takes into account the errors in the independent variable (i.e. discharge values) associated with measurement errors of flow path geometry, as these measurements were used for estimating the discharge using conveyance concept approximation.

Hydraulic friction

Equation 31 corroborates the suggestion by Hessel *et al.* (2003) that slope and hydraulic friction are positively correlated, although adding the slope variable to Equation 31 increased the prediction of f by only 5%. Hessel *et al.* (2003) show that in their cropland data, the slope variable explained up to 70% of the variation of hydraulic friction. This might be explained by the fact that their study sites had low vegetation cover which reduced the effect of the other factors on hydraulic roughness. Since the vegetation and rock cover are included in Equation 31, the hydraulic friction variation due to slope term might be explained by the variation of soil grain roughness or random roughness within the slope gradient. Such dependency of rill bed roughness on slope angle was shown in a study by Giménez and Govers (2001) where bed roughness amplitude increased significantly with slope.

Equation 31 shows that the basal plant cover term has the greatest effect on total friction. For instance, an increase of vegetation cover would add about 40% more in the logarithm of hydraulic friction than the same increase in rock cover. This conclusion of the partitioning process in some way agrees with Prosser *et al.*'s (1995) suggestion that, on densely grassed surfaces, a high percentage of the flow resistance is exerted by plant stems. In addition, greater root density associated with increasing basal plant cover adds to flow resistance (De Baets *et al.*, 2006; De Baets and Poesen, 2010). The existence of vegetation cover is essential in characterizing the hydraulics of the concentrated flow, whether it is in the bed of the flow path or not, as it influences the ability of concentrated flow to be formed, and controls the direction of flow paths, which will affect other roughness elements such as tortuosity.

Our hydraulic friction equation differs from a previous approach by Weltz *et al.* (1992) where each portion of the total friction was represented individually in an empirical equation, while the total friction factor was the result of adding up all the portions in one equation. Part of the reason for this may be due to the fact that the Weltz *et al.* (1992) equations were developed from data with a narrower range of slopes (4·2–12·9%) and their equation was developed for overland flow regardless of whether the flow was concentrated or sheet flow. The approach of using the friction factor to predict velocity has been criticized for the fact that it has been used without taking into the account the temporal and spatial variability of hydraulic roughness (Govers *et al.*, 2000; Smith *et al.*, 2007).

The equations presented here are capable of capturing both spatial and temporal variability in hydraulic roughness. For example, the effects of cover removal (fire or other disturbance) on hydraulic roughness are accounted for by having vegetation and rock cover terms in Equation 31. Spatial and temporal variability in hydraulic roughness are further explained in Equation 31 through the discharge term. Temporal fluctuations and spatial variability in discharge over consistent vegetation and cover values yield concomitant hydraulic roughness adjustments. The slope term also imparts capability to detect, under similar cover conditions, variations in hydraulic roughness with spatial variations in hillslope angle. Therefore, these new equations are robust not only in the range of conditions from which they are derived, but also in their capability to capture spatial and temporal fluctuations in the friction factor.

Flow path widths

The results of this study show that concentrated flow path widths were generally wider than cropland rills for the same flow discharge. Both constants of Equation 36 are significantly ($\alpha = 0{\cdot}05$) different than the results of Gilley *et al.* (1990) from croplands (see Figure 5). This result was even more evident when using RMA regression for developing the equation. Using the Breaks site data, Moffet *et al.* (2007) found that only the constant value '*a*' was significantly different from Gilley *et al.* (1990). Our results using data from diverse rangelands indicate that both constants *a* and *b* were significantly different relative to the constants proposed by Gilley *et al.* (1990). The difference between Equation 36 and that of Gilley *et al.* (1990) can be explained by the fact that sloping rangeland sites have relatively shallow soils which forces the concentrated flow path to spread wider as flow discharge increases.

In addition, as Equation 37 implies, hillslopes with higher percentage of bare soil or less plant residue would form narrow concentrated flow paths. The equation concurs with the fact that bare soil percentage is correlated negatively with the

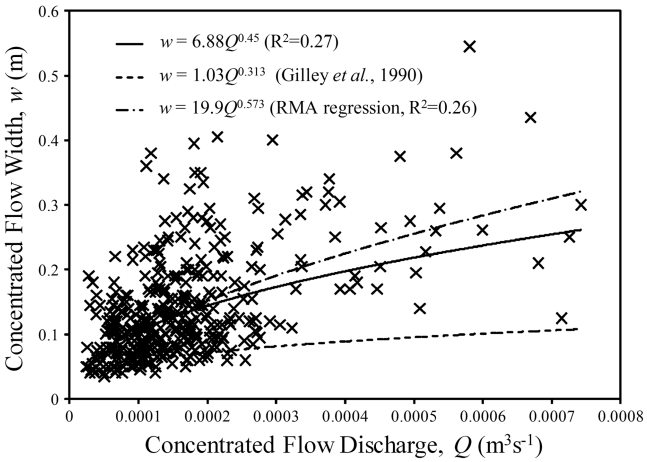

Figure 5. Power relationship for concentrated flow width as a function of flow discharge compared to relationships developed for cropland.

friction factor and positively with velocity. High velocity flow tends to be concentrated whereas low velocity flow tends to disperse. These relationships are evident as flow width was significantly lower on burned than unburned sites. The narrowest flow paths were obtained from experiments performed immediately post-fire, and burned sites formed more concentrated flow paths than unburned sites (Table IX).

Equations robustness

The resulting predictive equations of this study for concentrated flow velocity (Equations 27 and 28), hydraulic friction (Equations 31 and 32), and width (Equations 33 and 37) represent a diverse set of rangeland environments. The input variables that are required to apply these equations can be obtained from readily measureable hillslope characteristics, which are routinely collected by rangeland managers and researchers. The predictive equations developed could potentially be improved by including more variables like soil texture, organic matter content, root density, and random roughness, however, these variables are not as commonly measured/reported by rangeland managers and researchers as those used in this study.

As was seen in Table VII, the equations responses do not radically deviate from the range of the experimental observations even in the cases of running the equations by combining boundary values of all input variables. Although the results from Equation 27 showed higher RMSE than those of the model where Equation 31 was substituted into Equation 8, the fact that R^2 values for Equations 27 and 31 were almost the same showed an advantage of using Equation 27 for predicting flow velocity directly without the need for using additional equations. What also makes Equation 31 less advantageous than Equation 27 is its need for an R_h estimate, which raises the level of parameter induced model uncertainty. However, Equation 31 can be used for the partitioning process of the friction factor, which is important for the erosion model component in physically-based water erosion models such as Rangeland Hydrology and Erosion Model (RHEM) (Nearing *et al.*, 2011). For instance, in Equation 31 each vegetation cover term could be understood as its friction contribution to the total friction factor. The intercept in the equation could be assumed to be the friction factor due to soil grains and random roughness, while the flow discharge still explains some of the temporal variability of the hydraulic roughness. Equation 31 would be more effective in tracking the temporal and spatial variability of hydraulic roughness when the temporal variability of flow discharge and the spatial variability of slope are available. Equation 31 can be replaced by Equation 32 in the case where only bare soil percentage is available and the fractions of the attributes of ground cover are not available.

Finally, paired *t*-test showed that the response of the resulting predictive equations and the observations with one concentrated flow path are not significantly different at $\alpha = 0{\cdot}05$. This indifference supports the validity of using the conveyance concept for distributing the flow discharge into several flow paths.

Table IX. Average flow path width and number of flow paths for each treatment.

Site treatment	Number of observations	Flow path width (cm)	Number of flow paths
Burn year 0	84	10·0	2·3
Burn year 1	93	11·1	2·4
Burn year 2	57	14·1	2·7
Burn year 3	60	15·6	3·1
Unburned	97	19·7	1·9

Conclusions

In this paper, we examine the hydraulics of concentrated flow using unconfined field experimental data over diverse rangeland landscapes, and develop new empirical prediction models for different rangeland concentrated flow hydraulic parameters. The models are applicable across a wide span of rangeland sites, soil, and vegetation and ground cover conditions.

The overall hydraulic characteristics in which concentrated flow forms on rangelands differ significantly from that of cropland rills. The complexity of ground cover in rangeland landscapes relative to cropland adds more factors that control the hydraulics of concentrated flow. The morphology of rangeland vegetation, particularly grasses, and the shallowness of soil layers in rangelands force the concentrated flow path to go wider rather than deeper as flow discharge increases. In such conditions, the increase of flow discharge increases the ground and vegetation cover that flow encounters and consequently increases the hydraulic friction. Thus, velocity would be overestimated if predicted using discharge alone.

Concentrated flow on rangelands is also controlled by slope, particularly on newly disturbed sites. These sites have a high percentage of bare soil and insufficient vegetation and rock cover to counteract the driving force of gravity for the flow. Moreover, slope has an effect on the rock and vegetation cover which are important controllers of concentrated flow. For instance, within the scope of the data of this study, rock cover decreased as slope increased in sites with little vegetation cover. In such sites, velocity increased as slopes increased not only because of the increase of gravitational forces, but also due to the lack of rock cover. However, the negative correlation between rock and slope would be expected to hold until erosion of the newly disturbed site exposes subsurface rocks.

The resulting predictive equations of this study for concentrated flow velocity ($R^2 = 0{\cdot}47$), hydraulic friction ($R^2 = 0{\cdot}52$), and width ($R^2 = 0{\cdot}4$) represent a diverse set of rangeland environments. The velocity equation was obtained from a velocity data set that ranged from 0·019 to 0·45 $m\,s^{-1}$. The hydraulic friction equation was obtained from a friction factor data set that ranged from 0·43 to 1480. The width equation was obtained from a width data set that ranged from 3·5 to 54·5 cm.

The ground cover variables that are required to apply these equations are readily available from ecological sites, soils, and vegetation characteristics. Such data are routinely collected by range managers and scientists. Thus, these predictive equations can be robustly applied for estimating concentrated flow hydraulic parameters as inputs for hydrologic models of diverse rangeland ecosystems.

Acknowledgments—The authors wish to thank the Natural Resources Conservation Service for funding of this project as part of the Grazing Lands component of the Conservation Effects Assessment Project (CEAP). The authors also wish to express appreciation to the Joint Fire Science Program for funding the fieldwork associated with this project. Portions of the field research were funded by Joint Fire Science Program grants for investigating fire effects on rangeland runoff and erosion processes. The authors would also like to thank their parents for providing the nurturing environments and emotional support so necessary for becoming successful in our chosen and challenging scientific careers. Field studies at pinyon and juniper woodland sites in this project are part of the Sagebrush Treatment Evaluation Project (SageSTEP) funded by the US Joint Fire Science Program. This is Contribution Number 53 of the SageSTEP project. USDA is an equal opportunity provider and employer.

References

Abrahams AD, Parsons AJ, Luk S. 1990. Field experiments on the resistance to overland flow on desert hillslopes, erosion, transport and deposition processes. In *Proceedings of the Jerusalem Workshop*, March–April 1987, IAHS 189. IAHS Press: Wallingford.

Abrahams AD, Li G, Parsons AJ. 1996. Rill Hydraulics on semi-arid hillslope, southern Arizona. *Earth surface processes Landforms* **21**: 35–47.

Allison PD. 1999. *Multiple Regression: A Primer*. Pine Forge Press: Newbury Park, CA.

De Baets S, Poesen J. 2010. Empirical models for predicting the erosion-reducing effect of plant roots during concentrated flow. *Geomorphology* **118**: 425–432.

De Baets S, Poesen J, Gyssels G, Knapen A. 2006. Effects of grass roots on erodibility of topsoils during concentrated flow. *Geomorphology* **76**: 54–67.

Flerchinger GN, Cooley KR. 2000. A ten-year water balance of a mountainous semi-arid watershed. *Journal of Hydrology* **237**: 86–99.

Foster GR, Huggins LF, Meyer LD. 1984a. A laboratory study of rill hydraulics: I. Velocity relationships. *Transactions of the American Society of Agricultural Engineers* **27**(3): 790–796.

Foster GR, Huggins LF, Meyer LD. 1984b. A laboratory study of rill hydraulics: II. Shear stress relationships. *Transactions of the American Society of Agricultural Engineers* **27**(3): 797–804.

Gilley JE, Weltz MA. 1995. Hydraulics of overland flow. In *USDA – Water Erosion Prediction Project: Hillslope Profile and Watershed Model Documentation*, Flanagan DC, Nearing MA (eds), NSERL Report 10. National Soil Erosion Research Laboratory: West Lafayette, IN; chapter 10.

Gilley JE, Kottwitz ER, Simanton JR. 1990. Hydraulic characteristics of rills. *Transactions of the American Society of Agricultural Engineers* **33**: 1900–1906.

Giménez R, Govers G. 2001. Interaction between bed roughness and flow hydraulics in eroding rills. *Water Resources Research* **37**: 791–799.

Giménez R, Planchon O, Silvera N, Govers G. 2004. Longitudinal velocity patterns and bed morphology interaction in a rill. *Earth Surface Processes and Landforms* **29**: 105–114. DOI. 10.1002/esp.1021.

Govers G. 1992. Relationships between discharge, velocity and flow area for rills eroding loose, non-layered materials. *Earth Surface Processes and Landforms* **17**: 515–528.

Govers G, Takken I, Helming K. 2000. Soil roughness and overland flow. *Agronomie* **20**: 131–146.

Grant GE. 1997. Critical flow constrains flow hydraulics in mobile-bed streams: a new hypothesis. *Water Resources Research* **33**: 349–358.

Hessel R, Jetten V, Guanghui Z. 2003. Estimating Manning's *n* for steep slopes. *Catena* **54**, 77–91. DOI. 10.1016/S0341-8162(03)00058-4.

Julien PY, Simons DB. 1985. Sediment transport capacity of overland flow. *Transactions of the American Society of Agricultural Engineers* **28**(3): 755–762.

Lane LJ, Foster GR. 1980. Concentrated flow relationships. In *CREAMS: A Field-scale Model for Chemicals, Runoff, and Erosion from Agricultural Management Systems*, Knisel W (ed.), US Department of Agriculture, Conservation Research Report **26**. US Department of Agriculture: Washington, DC; 474–485.

Line DE, Meyer LD. 1988. Flow velocities of concentrated runoff along cropland furrows. *Transactions of the American Society of Agricultural Engineers* **31**(5): 1435–1439.

McIver JD, Brunson M, Bunting S, Chambers J, Devoe N, Doescher P, Grace J, Johnson D, Knick S, Miller R, Pellant M, Pierson F, Pyke D, Rollins K, Roundy B, Schupp G, Tausch R, Turner D. 2010. *SageSTEP: A Region-wide Experiment to Evaluate Effects of Fire and Fire Surrogate Treatments in the Sagebrush Biome, RMRS-GTR-237*. US Department of Agriculture, Forest Service: Fort Collins, CO.

Moffet CA, Pierson FB, Robichaud PR, Spaeth KE, Hardegree SP. 2007. Modeling soil erosion on steep sagebrush rangeland before and after prescribed fire. *Catena* **71**(2): 218–228. DOI. 10.1016/j.catena.2007.03.008.

Nearing MA, Foster GR, Lane LJ, Finkner SC. 1989. A processed based soil erosion model for USDA-water erosion prediction project technology. *Transactions of the American Society of Agricultural Engineers* **32**(5): 1587–1593.

Nearing MA, Norton LD, Bulgakov DA, Larionov GA, West LT, Dontsova KM. 1997. Hydraulics and erosion in eroding rills. *Water Resources Research* **33**: 865–876.

Nearing MA, Simanton JR, Norton LD, Bulygin SY, Stone J. 1999. Soil erosion by surface water flow on a stony, semiarid hillslope. *Earth Surface Processes and Landform* **24**: 677–686.

Nearing MA, Wei H, Stone JJ, Pierson, Spaeth KE, Weltz MA, Flanagan DC, Hernandez M. 2011. A Rangeland Hydrology and Erosion Model. *Transactions of the American Society of Agricultural and Biological Engineers* **54**: 901–908.

Pierson FB, Spaeth KE, Weltz MA, Carlson DH. 2002. Hydrologic response of diverse western rangelands. *Journal of Range Management* **55**: 558–570.

Pierson FB, Bates JD, Svejcar TJ, Hardegree SP. 2007. Runoff and erosion after cutting western juniper. *Rangeland Ecology and Management* **60**: 285–292.

Pierson FB, Robichaud PR, Moffet CA, Spaeth KE, Hardegree SP, Clark PE, Williams CJ. 2008. Fire effects on rangeland hydrology and erosion in a steep sagebrush-dominated landscape. *Hydrological Processes* **22**: 2916–2929. DOI. 10.1002/hyp.6904.

Pierson FB, Moffet CA, Williams CJ, Hardegree SP, Clark P. 2009. Prescribed-fire effects on rill and interrill runoff and erosion in a mountainous sagebrush landscape. *Earth Surface Processes and Landforms* **34**: 193–203.

Pierson FB, Williams CJ, Kormos PR, Hardegree SP, Clark PE. 2010. Hydrologic vulnerability of sagebrush steppe following pinyon and juniper encroachment. *Rangeland Ecology and Management* **63**: 614–629. DOI. 10.2111/REM-D-09-00148.1.

Poesen JW, Wesemael BV, Bunte K, Benet AS. 1998. Variation of rock cover and size along semiarid hillslopes: a case study from southeast Spain. *Geomorphology* **23**: 323–335.

Prosser IP, Dietrich WE, Stevenson J. 1995. Flow resistance and sediment transport by concentrated overland flow in a grassland valley. *Geomorphology* **13**: 71–86.

Roels JM. 1984. Flow resistance in concentrated overland flow on rough slope surface. *Earth Surface Processes and Landforms* **9**: 541–551.

Romme WH, Allen CD, Bailey JD, Baker WL, Bestelmeyer BT, Brown PM, Eisenhart KS, Floyd ML, Huffman DW, Jacobs BF, Miller RF, Muldavin EH, Swetnam TW, Tausch RJ, Weisberg PJ. 2009. Historical and modern disturbance regimes, stand structures, and landscape dynamics in piñon-juniper vegetation of the western United States. *Rangeland Ecology and Management* **62**: 203–222.

Simanton JR, Renard KG, Christiansen CM, Lane LJ. 1994. Spatial distribution of surface rock fragments along catenas in semiarid Arizona and Nevada, USA. *Catena* **23**: 29–42.

Smith MW, Cox NJ, Bracken LJ. 2007. Applying flow resistance equations to overland flows. *Progress in Physical Geography* **31**(4): 363–387. DOI. 10.1177/0309133307081289

Takken I, Govers G, Ciesiolka CAA, Silburn DM, Loch RJ. 1998. *Factors Influencing the Velocity–Discharge Relationships in Rills*. IAHS Publication 249. IAHS Press: Wallingford; 63–69.

US Army Corps of Engineers. 1993. *HEC-2 Water Surface Profile. Users Manual*. US Army Corps of Engineers. Hydrologic Engineering Center: Davis, CA.

Weisheng X, Tingwu L. 2002. The elementary dynamics analysis of rill flow. *Proceedings, 12th ISCO Conference*, Beijing.

Weltz MA, Awadis AB, Lane LJ. 1992. Hydraulic roughness coefficients for native rangelands. *Journal of Irrigation and Draining Engineering, ASCE* **118**(5): 776–790.